National Defence / Défense nationale

REAL-TIME ANALYSIS OF A SPREAD SPECTRUM ENVIRONMENT WITH AN OPTOELECTRONIC CYCLIC CROSS CORRELATION: PROOF-OF-CONCEPT EXPERIMENTS (U)

by

N. Brousseau and J.W.A. Salt

DEFENCE RESEARCH ESTABLISHMENT OTTAWA
TECHNICAL NOTE 95-14

Canada

October 1995
Ottawa

National Defence
Défense nationale

REAL-TIME ANALYSIS OF A SPREAD SPECTRUM ENVIRONMENT WITH AN OPTOELECTRONIC CYCLIC CROSS CORRELATION: PROOF-OF-CONCEPT EXPERIMENTS (U)

by

N. Brousseau and J.W.A. Salt
EW Signal Processing Group
Electronic Support Measures Section

DEFENCE RESEARCH ESTABLISHMENT OTTAWA
TECHNICAL NOTE 95-14

PCN
05B02

October 1995
Ottawa

ABSTRACT

The purpose of this technical note is to present a new algorithm to obtain real-time information for electronic support measures for wideband, low probability of intercept radar and communication signals. This algorithm is Cyclic Cross Correlation(CCC). It allows the detection, separation and characterization of spread spectrum signals having overlapped spectra, the same carrier frequency and the same time of arrival. An optoelectronic real-time implementation of the CCC for large bandwidth, spread spectrum signals was constructed at the Defence Research Establishment Ottawa using an optical Time-Integrating Correlator(TIC). A description of the real-time optical implementation of the CCC with a TIC and the associated experimental results are presented. An assessment of the potential of this technique for application to radar and communication ESM is also included.

RESUME

Cette note technique présente un nouvel algorithme conçu pour extraire, en temps réel, de l'information de signaux de radar et de communication à large bande passante et à faible probabilité d'interception pour les mesures de soutien électronique. Il s'agit de l'intercorrélation cyclique (IC). Cet algorithme permet de séparer et de caractériser des signaux à spectre étalés ayant la même porteuse, le même temps d'arrivée et des spectres superposés. La mise en oeuvre optoélectronique, en temps réel de l'IC, par un Corrélateur à Intégration Temporelle (CIT) a été réalisée au Centre de recherche pour la défense, Ottawa, pour des signaux à spectre étalé à large bande passante. Ces travaux ainsi que les résultats expérimentaux obtenus sont présentés. Une évaluation du potentiel de cette technique pour application aux mesures de soutien électronique pour le radar et les communications est présentée.

EXECUTIVE SUMMARY

Cyclostationary processing techniques are emerging as powerful analysis tools for modern radar and communications spread spectrum Low Probability of Intercept (LPI) signals that use pseudo random sequences. These signals, either spread with sequences only or hybrids using time or frequency hopping combined with sequence spreading, are characterized by large bandwidths and low power spectral densities. This makes their detection by linear receivers such as spectral analysers very difficult. Non-linear receivers using cyclostationary processing have been proposed as a better approach to the detection and interception of these spread spectrum LPI signals because of their ability to sort the signals from the noise by using new parameters. However, the computer power required for a real time implementation of these algorithms for large bandwidth signals is prohibitive, even with the best digital systems available. Fortunately, it was recently demonstrated at NRL that acousto-optic wideband correlators substantially outperformed their digital counterparts. So harnessing the power of an optical correlator for the implementation of cyclo stationary signal processing is an exciting challenge that could lead to significant advancement.

The purpose of this technical note is to present a new algorithm to obtain real-time information for electronic support measures for wideband, low probability of intercept radar and communications signals. This algorithm is Cyclic Cross Correlation(CCC). It allows the detection, separation and characterization of spread spectrum signals having overlapped spectra, the same carrier frequency and the same time of arrival. A real-time optoelectronic implementation of the CCC for large bandwidth, spread spectrum signals was performed at the Defence Research Establishment Ottawa using an optical Time-Integrating Correlator(TIC). A description of the real-time optical implementation of the CCC with a TIC, and the associated experimental results are presented together with an assessment of the potential of this technique for radar and communication ESM. The definition of the CCC is introduced in Section 2 and followed by a description of a TIC in Section 3. A description of the implementation of the CCC with a TIC appears in Section 4 with experimental results in Section 5.

The real-time implementation of the CCC has great potential for the detection, characterization and direction finding of spread spectrum signals in a crowded, noisy environment where spectrum overlap is common and more than one signal may be associated with a particular carrier frequency and time difference of arrival. These features could be incorporated to design and implement advanced Electronic Support Measures against LPI spread spectrum signals used by some modern radar and communications systems.

TABLE OF CONTENTS

LIST OF FIGURES

LIST OF FIGURES

LIST OF ABBREVIATIONS

AWGN	=	Additive White Gaussian Noise
BPSK	=	Binary Phase Shift Keying
CCC	=	Cyclic Cross Correlation
DREO	=	Defence Research Establishment Ottawa
TDOA	=	Time Difference of Arrival
ESM	=	Electronic Support Measures
LPI	=	Low Probability of Intercept
RF	=	Radio Frequency
TIC	=	Time-Integrating Correlator

1.0 INTRODUCTION

Cyclostationary processing techniques are emerging as powerful analysis tools for modern radar and communications spread spectrum Low Probability of Intercept (LPI) signals that use pseudo random sequences. These signals, either spread only with sequences or hybrids using time or frequency hopping combined with sequence spreading, are characterized by large bandwidths and low power spectral densities. This makes their detection by linear receivers such as spectral analysers very difficult[1]. Non-linear receivers using cyclostationary processing have been proposed as a better approach to the detection and interception of these spread spectrum LPI signals because of their ability to sort the signals from the noise by using new parameters. However, the computer power required for a real time implementation of these algorithms for large bandwidth signals is prohibitive, even with the best digital systems available. Fortunately, it was recently demonstrated[2] at NRL that acousto-optic wideband correlators can substantially outperform their digital counterparts. The particular optoelectronic correlator presented in the NRL publication had a processing power of 10-12 Gflops and was equivalent to 25 to 60 VME boards. So harnessing the power of an optical correlator for the implementation of cyclo stationary signal processing is an exciting prospect that could lead to significant advancement.

The purpose of this technical note is to present a new algorithm to obtain real-time information for electronic support measures for wideband, low probability of intercept radar and communications signals. This algorithm is Cyclic Cross Correlation(CCC). It allows the detection, separation and characterization of spread spectrum signals having overlapped spectra, the same carrier frequency and the same difference of time of arrival. An real-time optoelectronic implementation of the CCC for large bandwidth, spread spectrum signals was constructed at the Defence Research Establishment Ottawa using an optical Time-Integrating Correlator(TIC). Optical TICs are analog computers designed primarily to perform the correlation of large bandwidth, long data streams. Applications such as DNA analysis[3], processing for code division multiple access signals and searches in large unstructured data bases have already been proposed for TICs. A description of the real-time optical implementation of the CCC with a TIC and the associated experimental results are presented. An assessment of the potential of this technique for radar and communications ESM applications is also included. It is demonstrated that the optoelectronic implementation of the CCC allows the real-time calculation of the CCC. Consequently, the separation and characterization of spread spectrum signals with overlapping spectra that share the same carrier frequency and the same time difference of arrival is achieved. An assessment of the potential of this technique for ESM on spread spectrum radar and communications signals is also included in the conclusion.

2.0 INTRODUCTION TO CYCLOSTATIONARY SIGNAL PROCESSING

Many signal processing techniques assume that both the signal and the noise are stationary. However, man-made signals such as radar and communications signals, usually contain parameters that vary periodically with time. The assumption of stationarity is then not valid. In order to better deal with these non stationary signals, W. Gardner et al.[2,4-11] have developed the theory of cyclostationary signal processing in which the periodicities of the signals are recognized and exploited by non-linear receivers. Therefore, the non-linear receivers based on cyclostationary processing are better suited for the detection and interception of non stationary signals.

Cyclostationary signal processing is a field of intense activity and numerous publications are available, including tutorials[9] and textbooks[10]. Applications have been proposed in the field of interception, signal feature detection and direction finding of weak man-made signals[4-13]. It also has been recognized[14-15] that many specialized transforms (often developed empirically) performed in the time or the frequency domain, such as the ambiguity function, the Wigner-Ville or the Choi-Williams distributions are cyclostationary processes. Optical implementations have been proposed for some of these processes such as the chip rate detector[16], the ambiguity function[17-19] and the cyclic spectrum[20].

2.1 The Cyclic Cross Correlation(CCC)

The particular cyclostationary process that will be focussed on here is the CCC. The CCC function, $R^{\alpha}_{s1s2}(\tau)$, is defined by

$$R^{\alpha}_{s1s2}(\tau) = \lim_{T\to\infty} \frac{1}{T} \int_{-T/2}^{T/2} s_1(t+\tau/2)\; s_2(t-\tau/2)\, e^{-i2\pi\alpha t}\, dt \qquad (1)$$

This is a crosscorrelation function where α is the cyclic frequency and where $s_1(t+\tau/2)$ and $s_2(t-\tau/2)$ are the signals received by two different antennas. The Fourier transform of the CCC, the cyclic spectral density function $S^{\alpha}_{s1s2}(f)$, is defined by

$$S^{\alpha}_{s1s2}(f) = \int_{-\infty}^{\infty} R^{\alpha}_{s1s2}(\tau)\; e^{-i2\pi f\tau}\, d\tau \qquad (2)$$

For α=0 it reduces to the conventional power spectral density function $S^{o}_{s1s2}(f)$.

Equation 1 can be interpreted[21] as the correlation between the RF signal $x(t+\tau/2)$ received by one antenna and the frequency shifted version $x(t-\tau/2)\ e^{-i2\pi\alpha t}$ of the same RF signal received by another antenna. It can be demonstrated that for cyclostationnary signals, a correlation exists between frequency shifted versions of the signal when the frequency shift is equal to one of the periodicities of the signal. This results from the periodical nature of the signal in time[9]. This property is an important means of distinguishing cyclostationary from stationary signals and noise. It also allows the detection of the signals and the characterization of their parameters.

2.2 Illustration of the Cyclic Cross Correlation

In order to help visualize the CCC and to understand its properties in terms of discriminating signals, a computer generated image has been produced (see Figure 1) that shows the CCC of three signals with overlapping spectra which share the same Time Difference of Arrival (TDOA) and the same carrier frequency. It illustrates the CCC of the three spread spectrum signals which have been used for the first set of experimental results of Section 5.1 of this Technical Note. The geometry of the location of the emitters of the three signals is illustrated in Figure 2 and their spectra are illustrated in Figure 3. These signals include two Binary Phase Shifted Keyed (BPSK) signals having the same TDOA of τ=0, the same carrier frequency but chip rates of 2 MHz and 5 MHz respectively. The third signal is a 30 MHz broadband source of Additive White Gaussian Noise (AWGN) located at a TDOA of τ=-1.46 μs. Figure 3a) and 3b) illustrate respectively the spectra of the 2 MHz and of the 5MHz BPSK signals. Figure 3c) illustrates the spectrum of the noise and Figure 3d) the spectrum of the sum of the three signals. The spectra of the three signals are overlapped and the BPSK signals have the same carrier frequency. The large amount of noise present makes the assessment of the situation very difficult if only conventional spectral analysis of the added signals is considered.

The CCC illustrated in Figure 1 shows many interesting features that are listed below. The horizontal plane of the CCC (Figure 1) contains the axis of the cyclic frequency α and, perpendicular to it is the TDOA τ. The amplitude of the CCC is represented (with a linear scale) on the vertical axis. It should be noted that:

1) the plane α=0 contains the conventional cross correlation of the signals. The peak N for the AWGN at τ=-1.46 μs and the peak A from the two BPSK signals at τ= 0 are separated by their different TDOA.

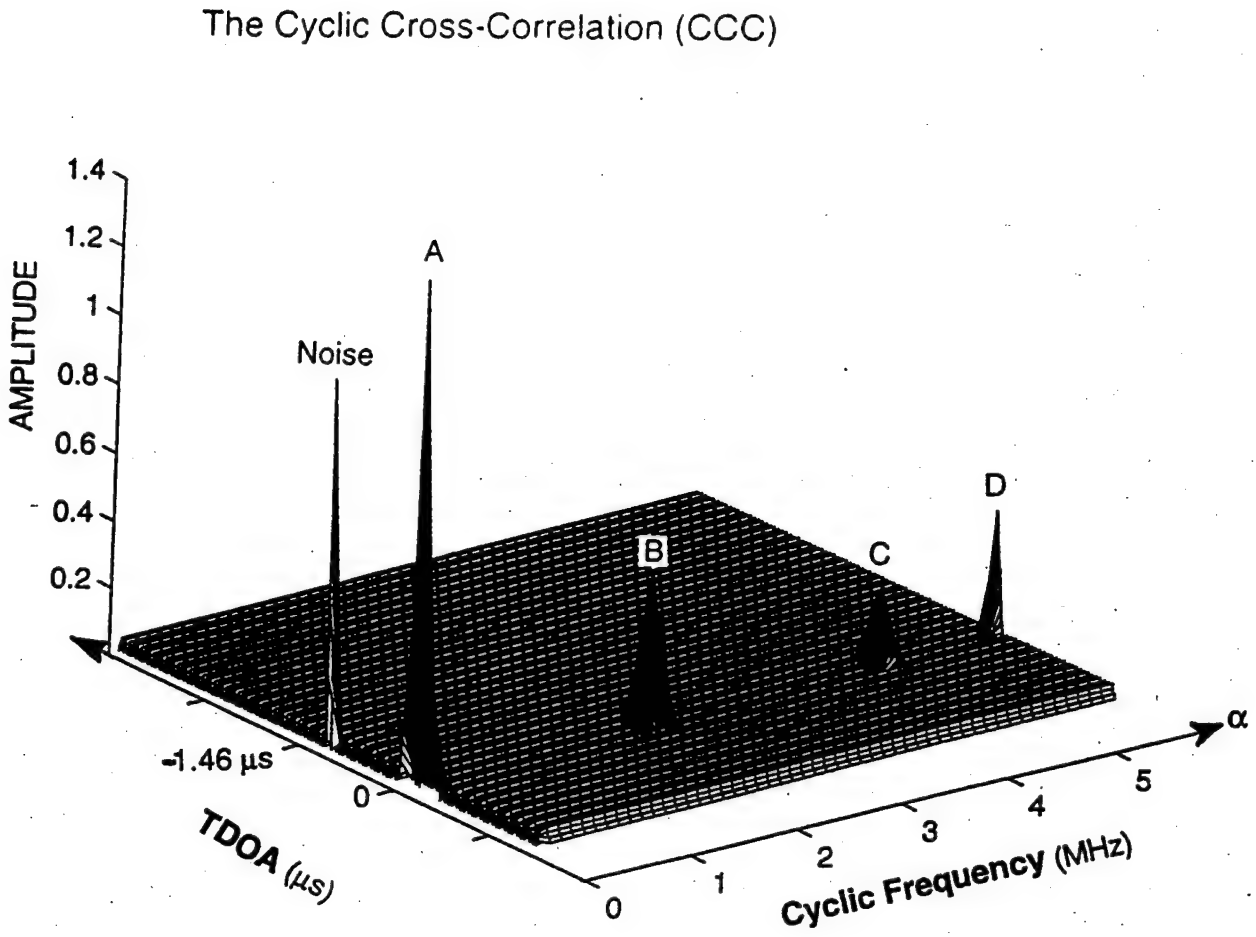

Figure 1: Three dimensional view of the CCC of three test signals.

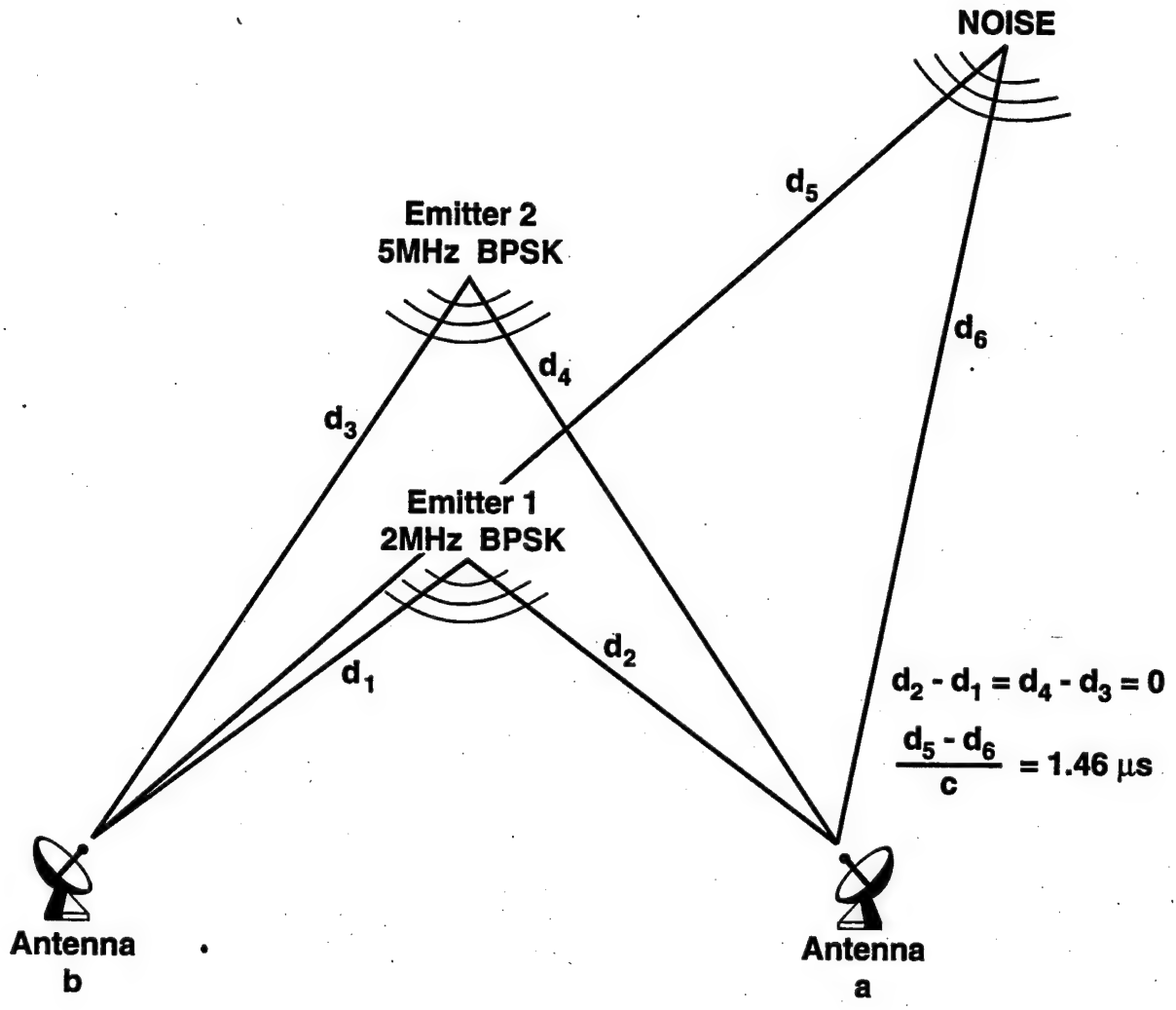

Figure 2: Geometry of the emitters:
emitter 1: 2 MHz BPSK with TDOA of 0
emitter 2: 5 MHz BPSK with TDOA of 0
emitter 3: AWGN with TDOA of -1.46 μs

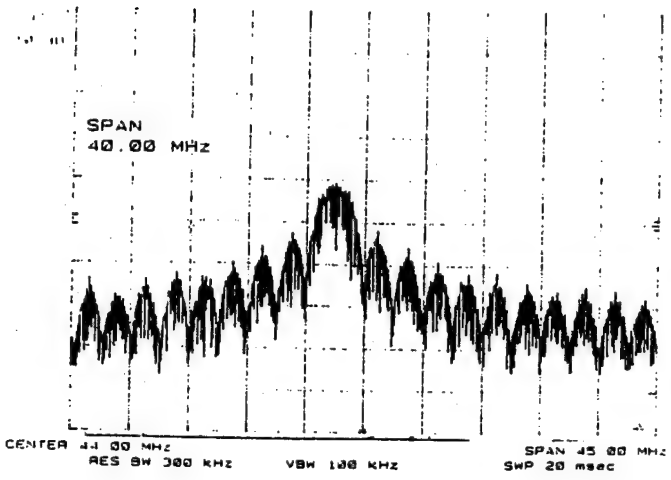

a) emitter 1: 2 MHz BPSK

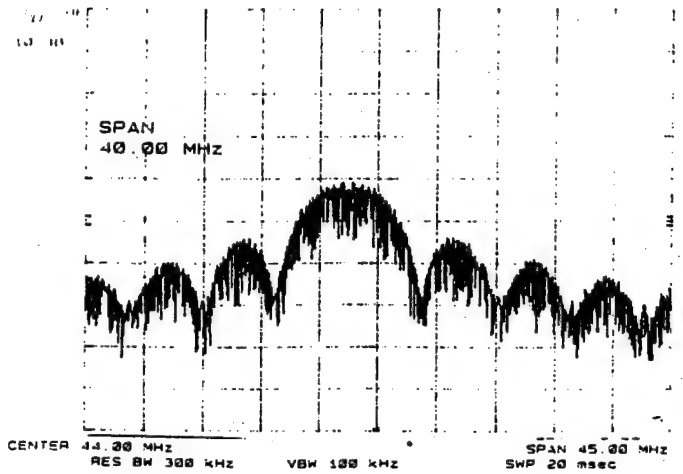

b) emitter 2: 5 MHZ BPSK

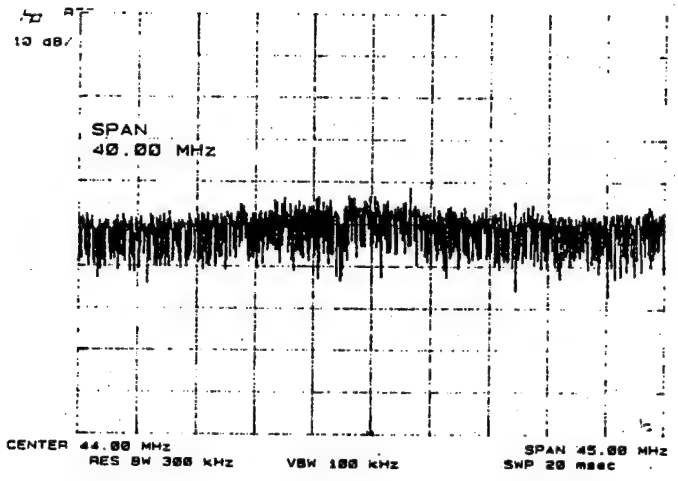

c) emitter 3: AWGN

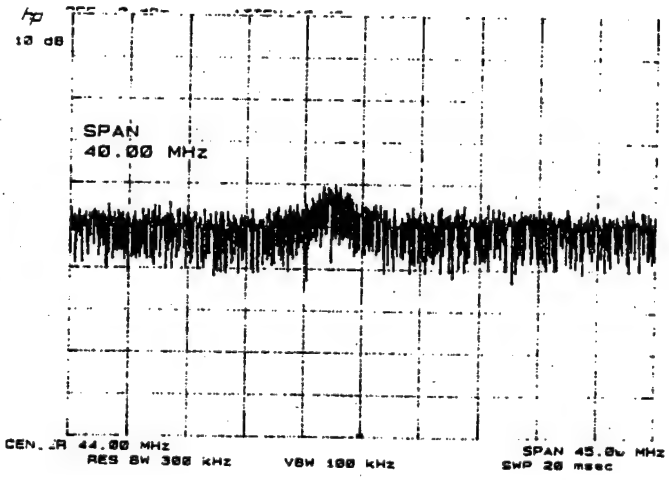

d) sum of the three emitters

Figure 3: Spectra of the signals of the three emitters:

2) it is impossible to separate, in the plane α=0, the correlation peaks of the two BPSK signals (peak A) as they share the same TDOA of 0 μs.

3) the correlation peak of the AWGN consists only of the thin peak N a τ=-1.46 μs and α=0. The small width of the peak is a direct consequence of the large bandwidth of the AWGN.

4) in the plane τ=0, four peaks appear. Peak A, at α=0, has already been mentioned and corresponds to the overlap of the autocorrelation of the two BPSK signals that share the same TDOA.

5) also at τ=0, peak B at α=2 MHz corresponds to the CCC of the 2 MHz BPSK signal and the peak C at α=4 MHz is a harmonic of the CCC of the same signal.

6) finally, peak D, at τ=0 and at α=5MHz, is produced by the CCC of the 5 MHz BPSK signal.

Figure 1 clearly demonstrates that the CCC has the capability to detect and separate, in the presence of a considerable amount of noise, spread spectrum signals having the same carrier frequency, overlapping spectra and the same TDOA. These features are of prime interest in the design of ESM systems for LPI radar and communications signals.

3.0 TIME-INTEGRATING CORRELATORS(TIC)

TICs are analog optical computers designed to perform the correlation of two signals. There are many ways to build optical time-integrating correlators. They are well documented in the literature [22-41] and good review papers are available[29,35,41]. The various factors affecting the performance of these systems have also been extensively studied[42-51]. A brief review of the principle of operation of these correlators is presented here, based on the tandem architecture described in [52] (Figure 4 and 5). The emphasis is on the characteristics and parameters that have an impact on the implementation of the CCC.

3.1 Description of the Optical Processor

The first operation performed by a TIC is the transformation of the RF signals, a(t) and b(t), to be correlated into light modulated beams. For the implementation of the CCC, the transmitted RF signals should be received by two separate antennas. The RF signals from each antenna are individually applied to one of the light modulators (Bragg cells). They consist of a piezoelectric transducer attached to a crystal in which acoustic waves are generated. As the acoustic waves propagate in the Bragg

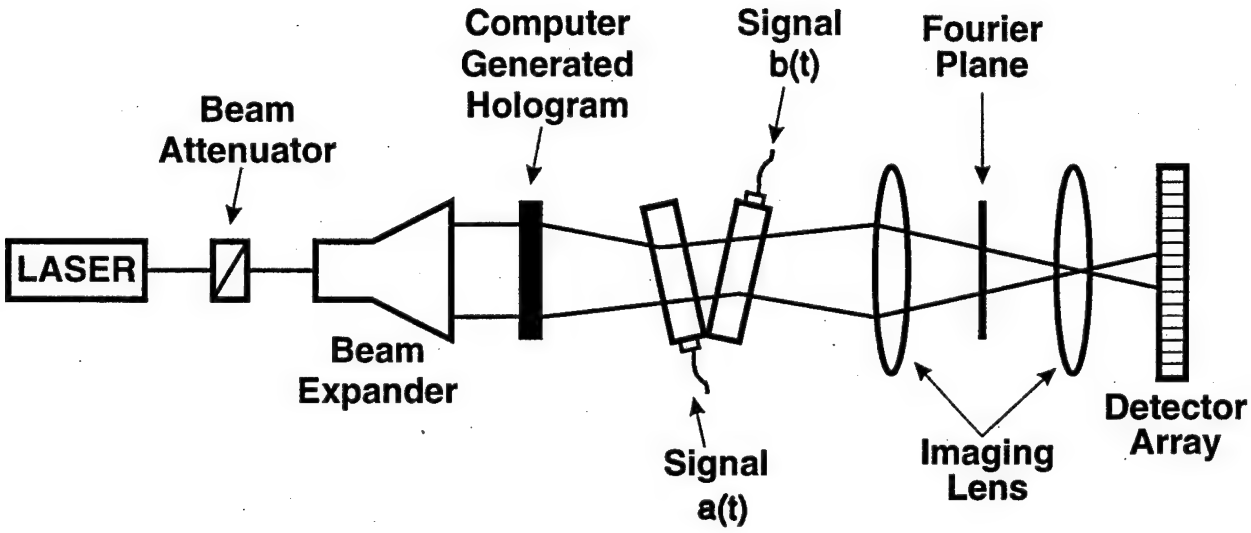

Figure 4: Time-integrating correlator.

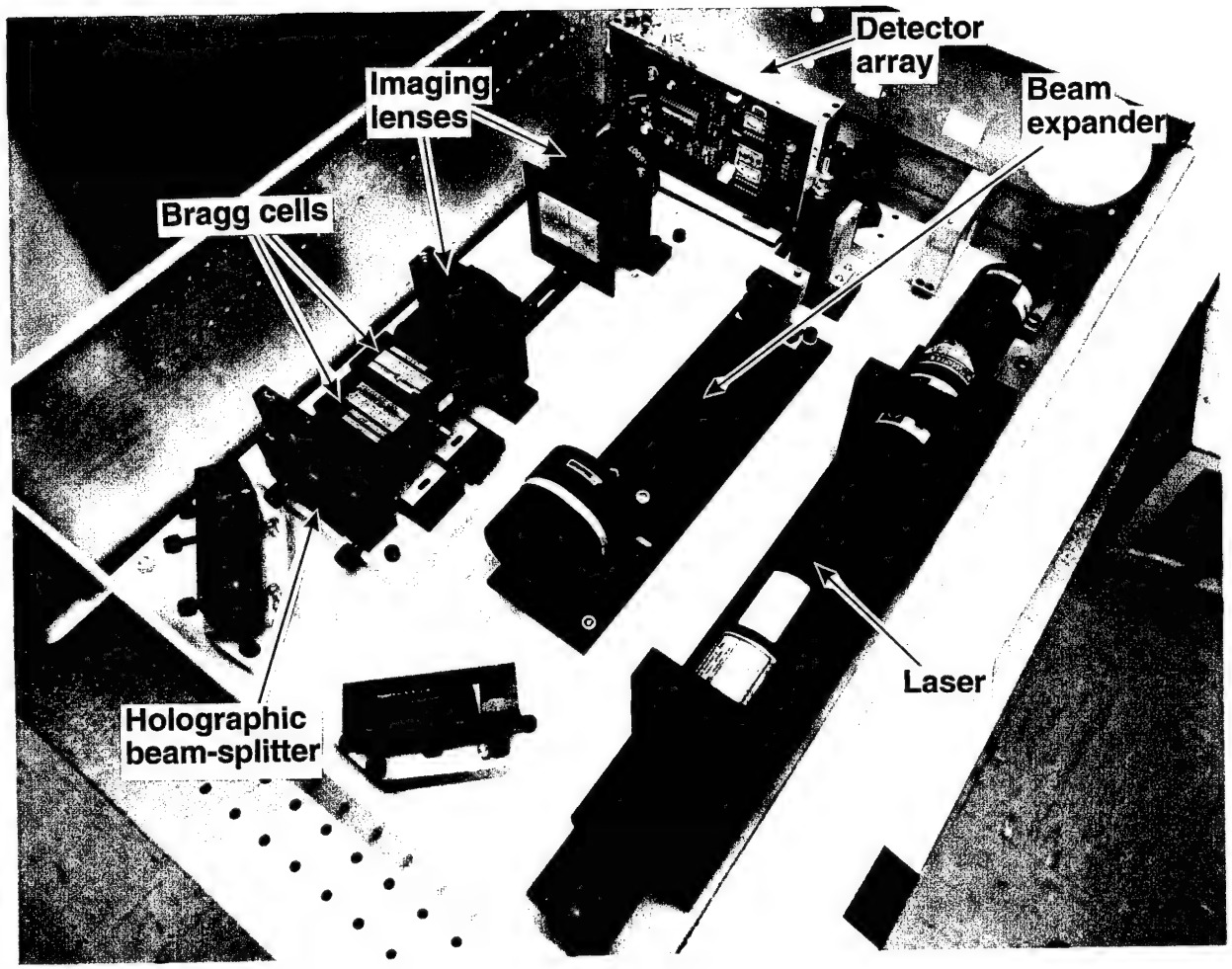

Figure 5: Photograph of a TIC mounted in a 19" rack.

cell crystals and a moving grating of changing indices of refraction is formed. The gratings in the Bragg cells are illuminated by two expanded laser beams originating from the same laser. Each beam interacts with the acoustic waves of only one Bragg cell. Some of the incident light is diffracted by the gratings and therefore, the information contained in the RF signals is simultaneously transferred to the diffracted laser beams. The signals propagating in each Bragg cell are physically oriented in opposite directions, a condition needed for the correlation. The gratings are imaged, with a lens, onto a detector array where they remain counterpropagating. The 5000-element detector array performs a time integration on the coherent addition of the two images of the signals.

If the variable z is the distance along the Bragg cells and their images, and if the origin z=0 is defined to be at the centre of the Bragg cells and, correspondingly at the centre of their images on the detector array, the optical signals diffracted by the Bragg cells are a(t+z/v) and b(t-z/v), where v is the velocity of propagation of the signals in the Bragg cells. The electrical signal produced by the detector array, s(t,z), is proportional to the square of the light distribution

$$s(t,z) = |a(t+z/v) + b(t-z/v)|^2 \quad (3)$$

$$= a^2(t+z/v) + b^2(t-z/v) + 2a(t+z/v)b(t-z/v) \quad (4)$$

A rigourous analysis using analytical functions can be found in [32]. Equation 4 is a simplification of these results. This response is then integrated for a duration T and the resulting signal S(T,z) is

$$S(T,z) = \int_T [a^2(t-z/v) + b^2(t-z/v) + 2a(t+z/v)\, b(t-z/v)]\, dt \quad (5)$$

The response of all the individual elements of the detector array is called a correlogram (see Figure 6). The third term of Equation 3 is the correlation of the input data a(t) and b(t). This correlation term is observed as a peak on a pedestal (generated by the first and second term of Equation 3). The presence of the peak indicates that the two input signals a(t) and b(t) are identical, conversely the absence of the correlation peak indicates that the two inputs are different.

A photo of a TIC is presented in Figure 5. Some of the advantages of this implementation is its relatively low volume that can be packaged into a 10 inch high space of a 19 inch rack. The

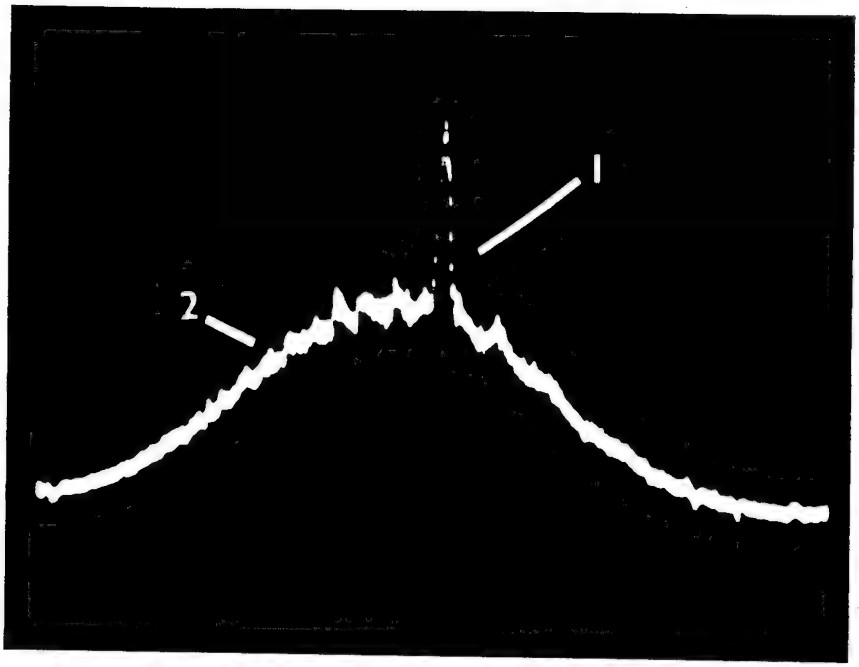

Figure 6: Correlation peak from a TIC.

power consumption is less than 500 Watts. The Bragg cells have a 30 MHz bandwidth centered at 45 MHz and make the TIC well suited for the processing of spread spectrum communications signals. The detector array has 5000 elements that can be read-out in 500 μs. The illumination is provided by a 20 mW helium-neon laser.

The TIC is run by a 486 personal computer whose main functions are to control the read-out of the detector array and to perform the removal of the pedestal (Figure 6) which facilitates the detection of the peak. Various techniques have been proposed and assessed at DREO[49] to perform pedestal removal. They all involved the subtraction of correlograms collected at different times. However, the time interval between the collection of the correlograms varies with the method. In order to deal with a tactical situation where the signal environment is likely to change rapidly, the method selected uses correlograms collected with the minimum time interval, that is successive correlograms. That particular method is described in[22,35,49].

Figure 7 illustrates the signal generation for the conventional operation of a TIC with the three signals described in section 2.0. The input to the TIC is made of the addition of two BPSK signals with chip rates of 2MHz and 5 MHz respectively, and AWGN whose spectra are illustrated in Figure 3. The two BPSK signals are added, and the combined signal is split. Similarly, the AWGN is split and a time delay of 1.46 μs is then introduced in one of the AWGN paths. The noise paths are then added to the BPSK signals and the two resulting signals are applied to the Bragg cells of the TIC for correlation. The geometry of the simulated signal sources is illustrated in Figure 2.

The correlation is formed on the detector array by an integration of duration T, calculated to provide sufficient processing gain to allow the detection of the correlation peaks. At the end of the integration time T, the correlation is already fully formed on the detector array and is clocked out. This leads to the real-time implementation of the CCC for a particular cyclic frequency α. In the system considered here, it takes a total of 500 μs to read the data from the 5000 elements of the detector array and access the CCC. However, the delay of 500 μs is not lost time, because the detector array is reset immediately after the transfer of the results to the device responsible for the clocking out and the next integration period starts during the clocking out of the results of the previous one.

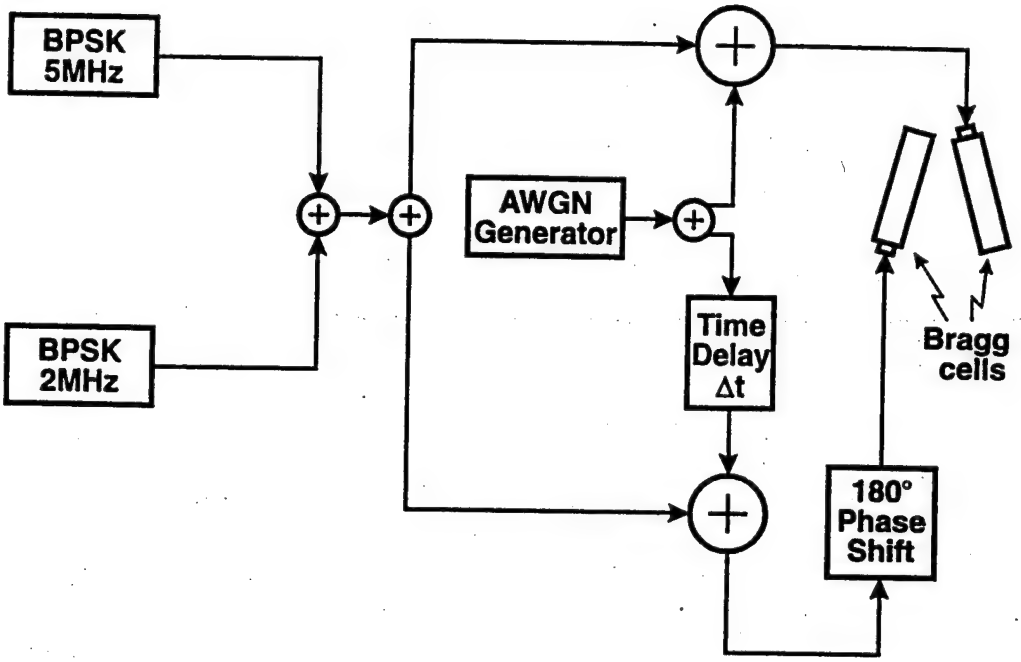

Figure 7: Generation of the input signals for the conventional operation of the correlator

4.0 IMPLEMENTATION OF THE CYCLIC AUTOCORRELATION WITH A TIME-INTEGRATING CORRELATOR

The implementation of the CCC, $R^{\alpha}_{s1s2}(\tau)$, is suggested by the interpretation of Equation 1 (presented in section 2.1) where the CCC is viewed as the correlation of one received RF signal with a frequency shifted version of the RF signal received by another antenna. Remembering that a TIC produces the correlation of all the signals that are applied to its Bragg cells, the CCC can be produced by frequency shifting the carrier frequencies of the two RF input signals by an appropriate amount before performing the correlation. A correlation peak appears when the difference of the carrier frequencies of the two signals is equal to one of the cyclic frequencies contained in the signals.

A schematic of the generation for a signal made of the addition of two Binary Phase Shift Keyed(BPSK) with a chip rate of 2 MHz and 5 MHz and AWGN is illustrated in Figure 8. The two BPSK signals are added, and the combined signal is split as in Figure 7. A time delay of 1.46 μs is then introduced in one of the AWGN paths. The noise paths are then added to the BPSK signals. The two resulting signals are then mixed with two different carrier frequencies (master and slave) and are applied to the Bragg cells of the TIC for correlation. The conventional cross correlation $R^{o}_{s1s2}(\tau)$ is produced when the two signals have the same carrier frequency. The CCC, for a cyclic frequency α, is produced when a frequency shift α has been applied to the carrier frequency of one of the received RF signals. In this system, changes in the carrier frequencies had to be made by hand. The TDOA window of the correlator used in this work was 89 μs, and was detected by a 5000-element array. It is possible, without using any special algorithm, to locate the center of a peak with a precision of 3 detector elements. The resulting resolution for the TDOA is 50 ns.

4.1 Bandwidth Limitations

The bandwidth of the Bragg cells incorporated in the TIC is 30 MHz, centered at a carrier frequency of 45 MHz. In order to optimize the use of this bandwidth, the CCC can be implemented by shifting the carrier frequency of the two signals by $\alpha/2$ and $-\alpha/2$ respectively rather than shifting the carrier of only one signals by α. This way, both signals have a carrier frequency at the same distance from the center frequency of the Bragg cells and the bandpass filtering resulting from the frequency response of the Bragg cells is the same for both signals. Correlation still appears in the CCC when the difference between the carrier of the two signals is equal to one of the cyclic frequencies of the signal.

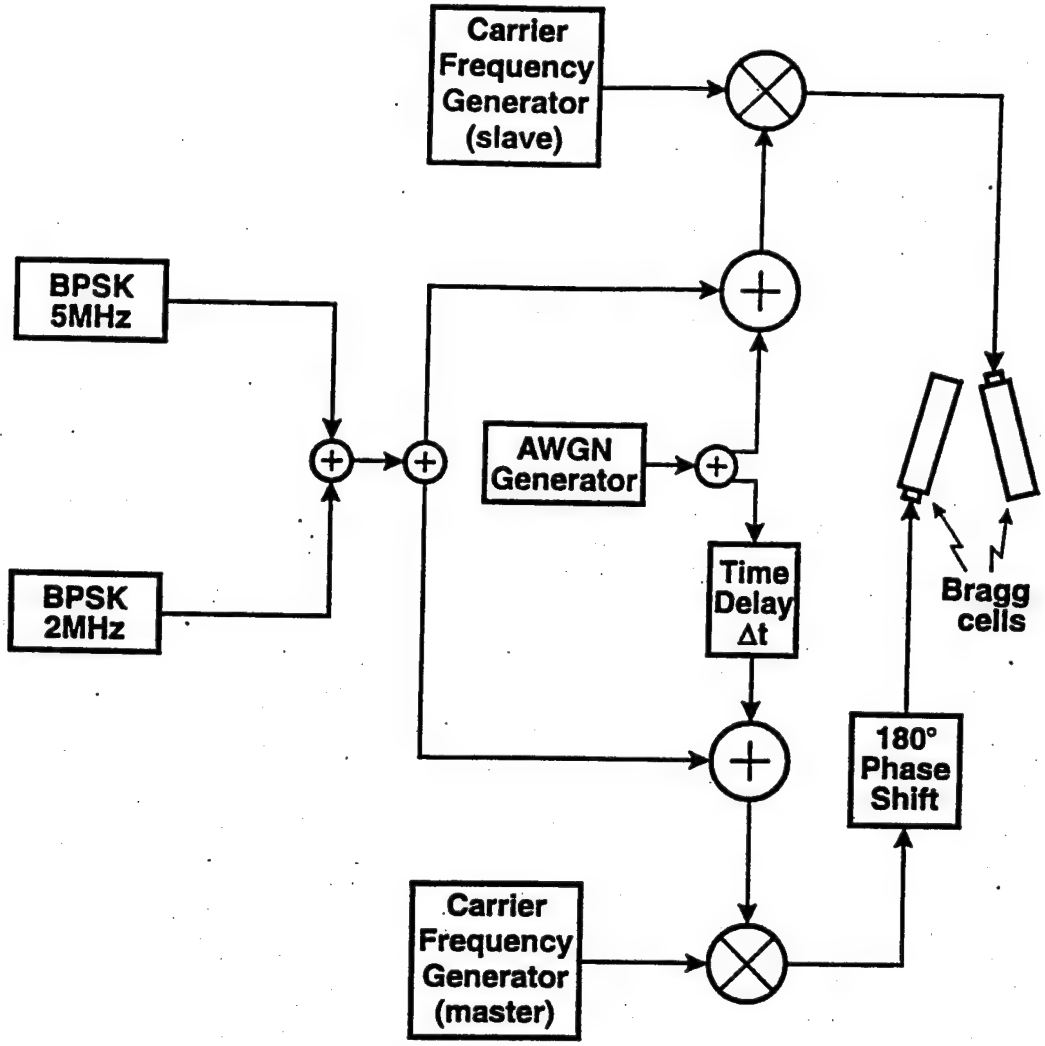

Figure 8: Generation of the input signals for the CCC.

5.0 EXPERIMENTAL RESULTS

The purpose of the proof-of-concept experiments was to demonstrate the capability of the CCC to discriminate between signals that could not be discriminated by a spectrum analyser and also that optical TIC can perform real-time calculation of the CCC of large bandwidth spread spectrum signals.

5.1 First Experiment

5.1.1 Simulated Signal Environment

The elements of the signal environment were selected to simulate a tactical situation involving three spread spectrum signals and to emphasize the capability of the CCC to discriminate between non-stationary signals occupying the same bandwidth and having the same TDOA and the same carrier frequency. The signal geometry is illustrated in Figure 2 and the spectra of the signals are illustrated in Figure 3. The detailed description of the signals and of the signal generation have already be presented in Sections 3.0 and 4.0 respectively.

The CCC for different cyclic frequencies can be produced by mixing different carrier frequencies to the signals before they are correlated by the TIC (see Figure 8). In our experiments, the values of these two carrier frequencies are adjusted by hand. When their difference is equal to one of the cyclic frequencies present in the input signals, a correlation peak appears in the output of the CCC. An automated scanning could be performed under computer control.

5.1.2 Cyclic Cross Correlation Results

Figure 9 contains the CCC of the three signals (described in section 4.0) for the cyclic frequency varying between α=0 and α=5 MHz, by steps of 1 MHz. The correlograms produced by the TIC are presented for each cyclic frequency α. The horizontal axis of each correlogram is labelled in number of detecting elements called pixels. This corresponds to the TDOA after calibration. The vertical axis (with a linear scale) is the amplitude of the CCC. Other interesting features can be observed in these correlograms:

1) Figure 9 a), for α=0, is the conventional cross correlation of the input signals. In this plane, the AWGN (Noise) and the two BPSK (peak A) are separated by their different TDOA. However, it is impossible to separate, for α=0, the two BPSK signals that share the same TDOA of 0 μs and produce superposed correlation peaks.

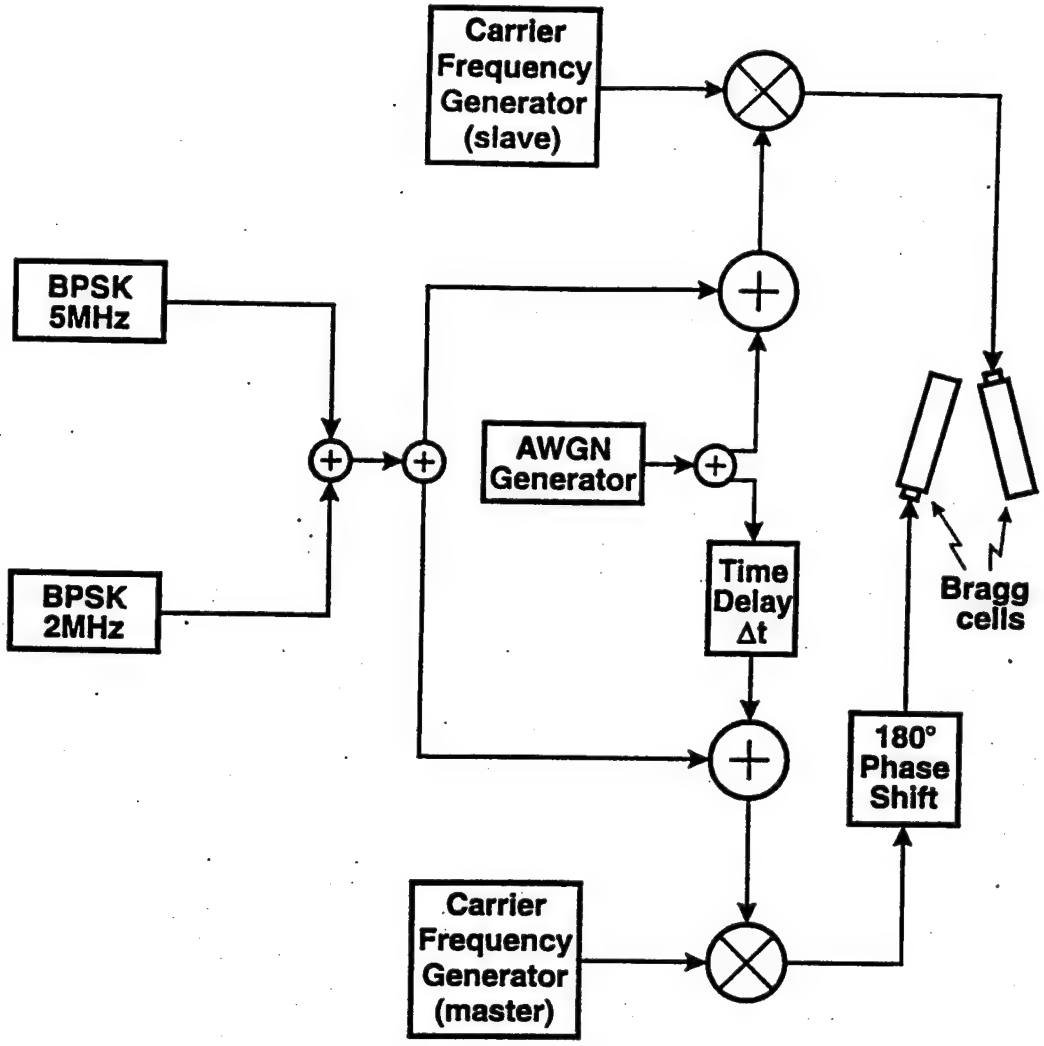

Figure 8: Generation of the input signals for the CCC.

5.0 EXPERIMENTAL RESULTS

The purpose of the proof-of-concept experiments was to demonstrate the capability of the CCC to discriminate between signals that could not be discriminated by a spectrum analyser and also that optical TIC can perform real-time calculation of the CCC of large bandwidth spread spectrum signals.

5.1 First Experiment

5.1.1 Simulated Signal Environment

The elements of the signal environment were selected to simulate a tactical situation involving three spread spectrum signals and to emphasize the capability of the CCC to discriminate between non-stationary signals occupying the same bandwidth and having the same TDOA and the same carrier frequency. The signal geometry is illustrated in Figure 2 and the spectra of the signals are illustrated in Figure 3. The detailed description of the signals and of the signal generation have already be presented in Sections 3.0 and 4.0 respectively.

The CCC for different cyclic frequencies can be produced by mixing different carrier frequencies to the signals before they are correlated by the TIC (see Figure 8). In our experiments, the values of these two carrier frequencies are adjusted by hand. When their difference is equal to one of the cyclic frequencies present in the input signals, a correlation peak appears in the output of the CCC. An automated scanning could be performed under computer control.

5.1.2 Cyclic Cross Correlation Results

Figure 9 contains the CCC of the three signals (described in section 4.0) for the cyclic frequency varying between α=0 and α=5 MHz, by steps of 1 MHz. The correlograms produced by the TIC are presented for each cyclic frequency α. The horizontal axis of each correlogram is labelled in number of detecting elements called pixels. This corresponds to the TDOA after calibration. The vertical axis (with a linear scale) is the amplitude of the CCC. Other interesting features can be observed in these correlograms:

1) Figure 9 a), for α=0, is the conventional cross correlation of the input signals. In this plane, the AWGN (Noise) and the two BPSK (peak A) are separated by their different TDOA. However, it is impossible to separate, for α=0, the two BPSK signals that share the same TDOA of 0 μs and produce superposed correlation peaks.

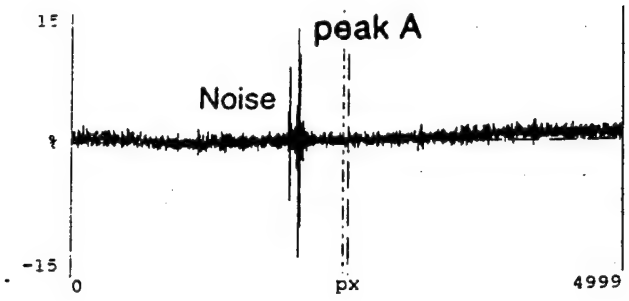

a) for α=0 MHz

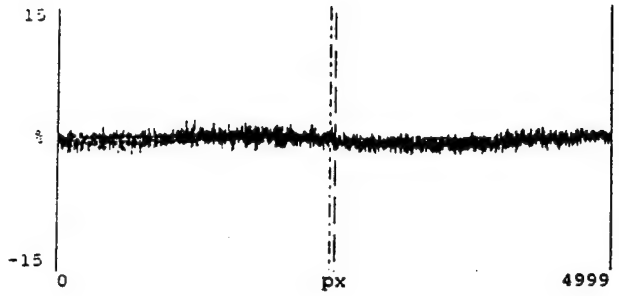

b) for α=1 MHz

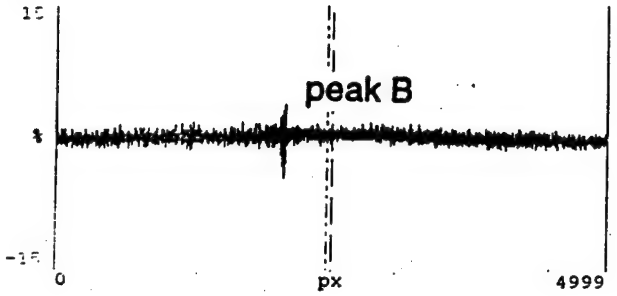

c) for α=2 MHz

d) for α=3 MHz

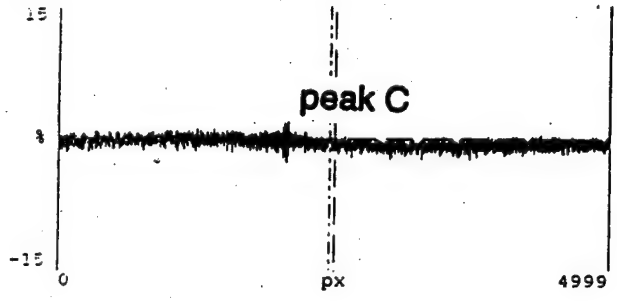

e) for α=4 MHz

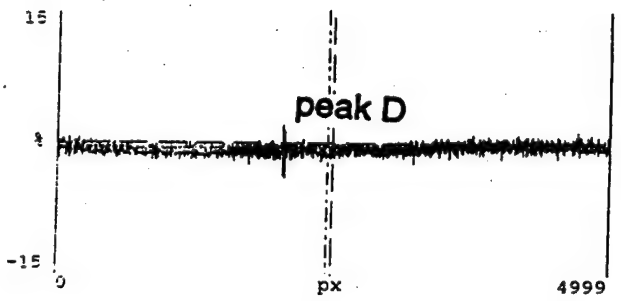

f) for α=5 MHz

Figure 9: Output of the optical correlator showing the CCC of the sum of the three signals of Figure 6 for different cyclic frequencies α

2) Figure 9 b) and 9 d) illustrates the CCC for α=1 MHz and α=3 MHz respectively. For these two cyclic frequencies, the AWGN and the BPSK signals do not produce any correlation peak.

3) For α=2 the CCC contains one peak (Figure 9c). Peak B is associated with the 2 MHz BPSK signal and is located at τ=0 μs. An harmonic of the CCC for the 2 MHz BPSK (peak C) can be found at α=4 MHz (Figure 9e).

4) Finally, for α=5 MHz (Figure 9f), peak D is produced by the 5 MHz BPSK signal at τ=0 μs.

Figure 1 is a synthesis of the results of Figure 9 and has been constructed from the experimental data collected in the work just described. It demonstrates clearly that the CCC has the capability to separate BPSK signals with overlapping spectra, sharing the same carrier frequency and the same TDOA, in the presence of a considerable amount of noise (equal to the power of the BPSK signals).

5.2 Second Experiment

5.2.1 Simulated Signal Environment

The capabilities of the TIC to produce in real-time the CCC of larger bandwidth signals has been explored by simulating the signal environment illustrated in Figure 10. In this case a 10 MHz BPSK, a 20 MHz BPSK and a source of AWGN share the same bandwidth, carrier frequency and TDOA. The spectra of the signals are illustrated in Figure 11. The schematic of the signal generation is similar to Figure 8 except that the long cable producing the time delay has been removed.

5.2.2 Cyclic Cross-Correlation Results

The results of the CCC for the cyclic frequency 0, 10 MHz, 20 MHz and 1 MHz are illustrated in Figure 12.

1) Figure 12 a) shows the CCC for α=0. The peak A is the superposition of the autocorrelation peak of the three signals present in the environment. The peak B is the superposition of the autocorrelation peaks of the emitters at 10 and 20 MHz while peak C is the autocorrelation peak of the emitter at 20 MHz.

2) Figure 12 b) shows the CCC for α=10 MHz. Peak D indicates the presence of an emitter at 10 MHz.

3) Figure 12 c) shows the CCC for α=20 MHz. Peak E indicate the presence of an emitter at 20 MHz.

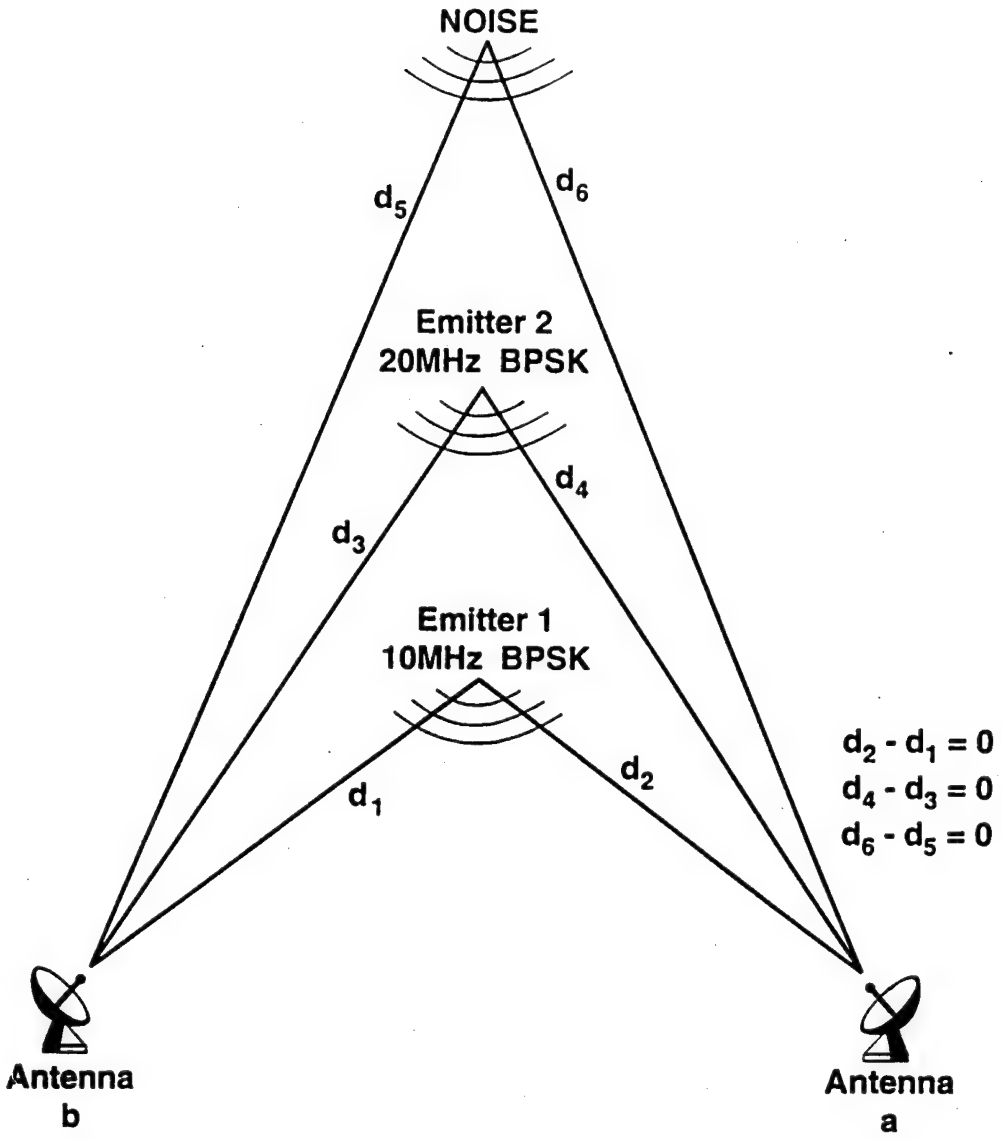

Figure 10: Geometry of the emitters
a) emitter 1: 10 MHz BPSK with TDOA of 0
b) emitter 2: 20 MHz BPSK with TDOA of 0
c) emitter 3: AWGN with TDOA of 0.

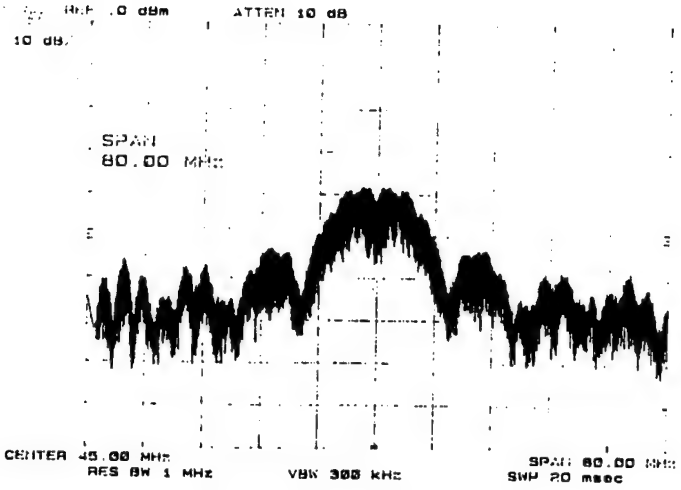

a) emitter 1: 10 MHz BPSK

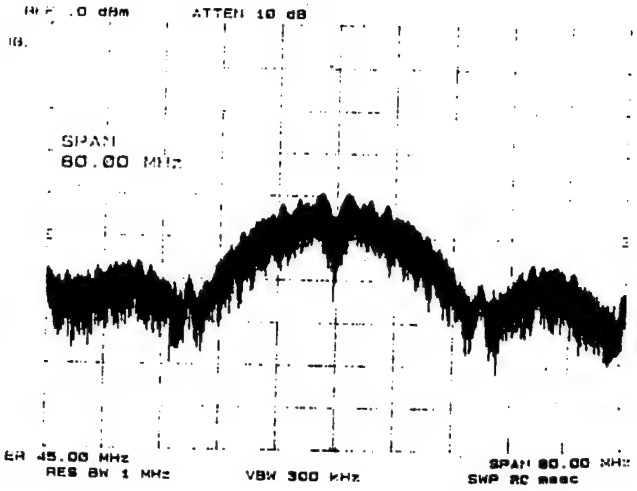

b) emitter 2: 20 MHz BPSK

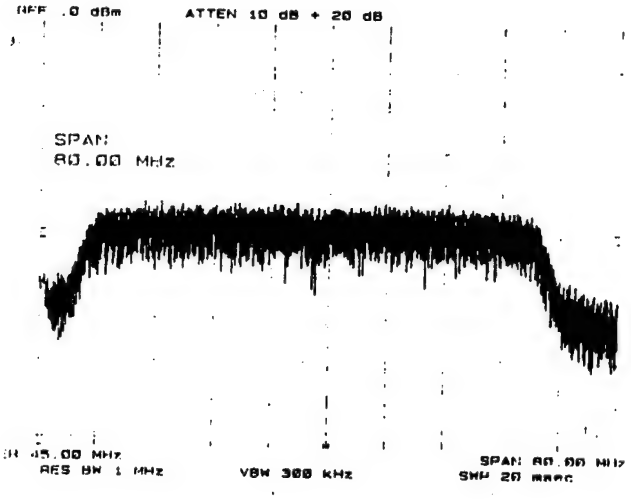

c) emitter 3: AWGN

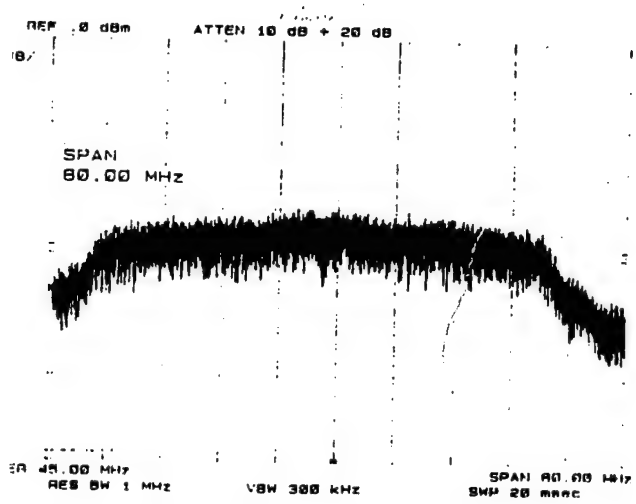

d) sum of the three emitters.

Figure 11: Spectra of the signals of the three emitters:

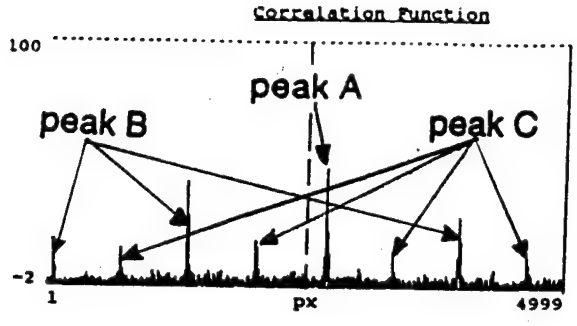

a) for α = 0 MHz

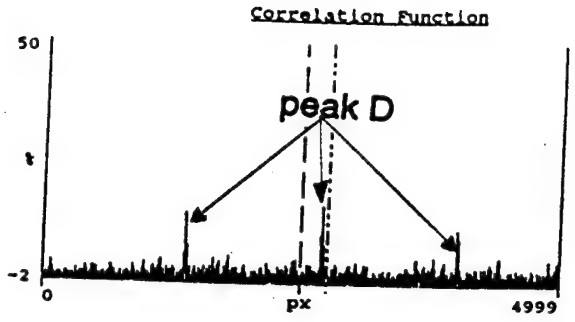

b) for α = 10 MHz

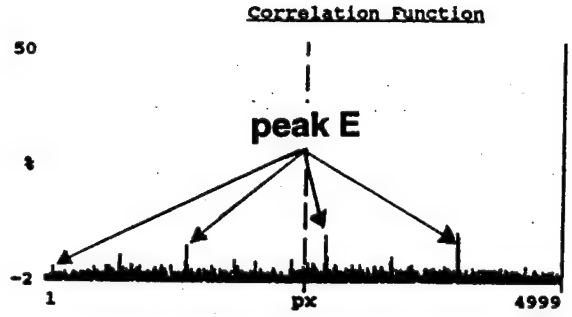

c) for α = 20 MHz

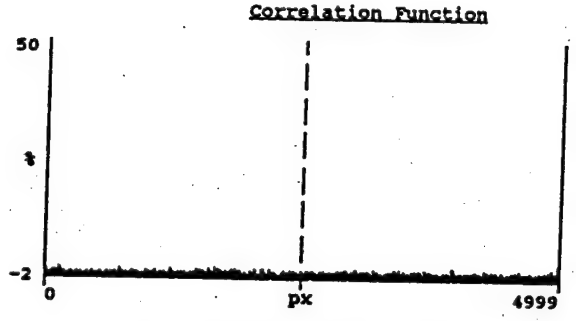

d) for α = 11 MHz.

Figure 12: Output of the optical correlator showing the CCC of the sum of the three signals of Figure 10

4) Figure 12 d, shows the CCC for α = 11 MHz. For this cyclic frequency, no peak is produced. Similar results are obtained for all cyclic frequencies that are different from 10 MHz and 20 MHz. It should be remembered that the bandwidth of the Bragg cells used in these experiments is only 30 MHz.

The experimental results of Figure 12 are presented as a 3-dimensional computer generated picture on Figure 13. This way to present the data emphasizes the capability of the CCC to detect and characterize large bandwidth spread spectrum signals even when a substantial amount of AWGN is located on the same TDOA.

All the experimental results presented in Figure 9 and 12 were obtained by letting the input signals flow through the Bragg cells for an integration time of 1000 μs. The CCCs for the particular cyclic frequency α considered were fully formed on the detector array at the end of the integration period leading to the real-time implementation of the CCC. The results were available 500 μs later after being clocked out of the detector array. The correlation peaks identified in Figure 9 and 12 are easily discernible from the noise and from each other. It would be possible to calculate the cyclic spectrum described by equation 2 by performing the Fourier transform of the CCC calculated by the TIC for the desired value of α.

5.3 Width of the Correlation Peaks on the Cyclic Frequency axis α

The width of the CCC peaks was experimentally measured by recording the amplitude of the peak as a function of the cyclic frequency. The results are illustrated in Figure 14 for a BPSK with a chip rate of 10 MHz. The amplitude of the peak decreases as the value of alpha gets away from the cyclic frequency of 10 MHz. The amplitude of the peak becomes null 500 Hz away from 10 MHz. However, a second lobe is observed between 500 Hz and 1000 Hz. No correlation peak was observed beyond 1000 Hz away from the chip rate of the BPSK. The width of the peaks produced by the other chip rate used in these experiments was identical.

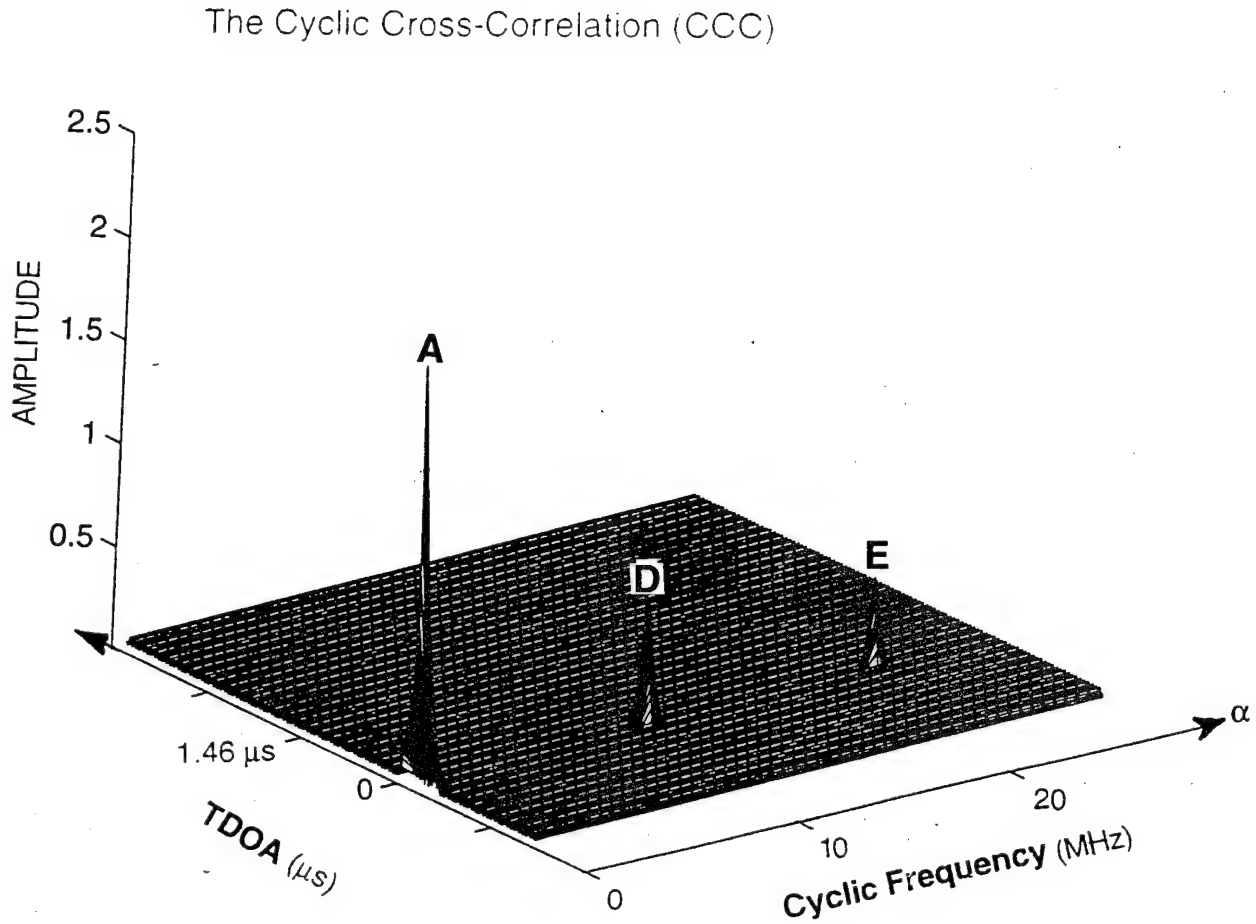

Figure 13: Three dimensional view of the CCC of the three test signals of Figure 10

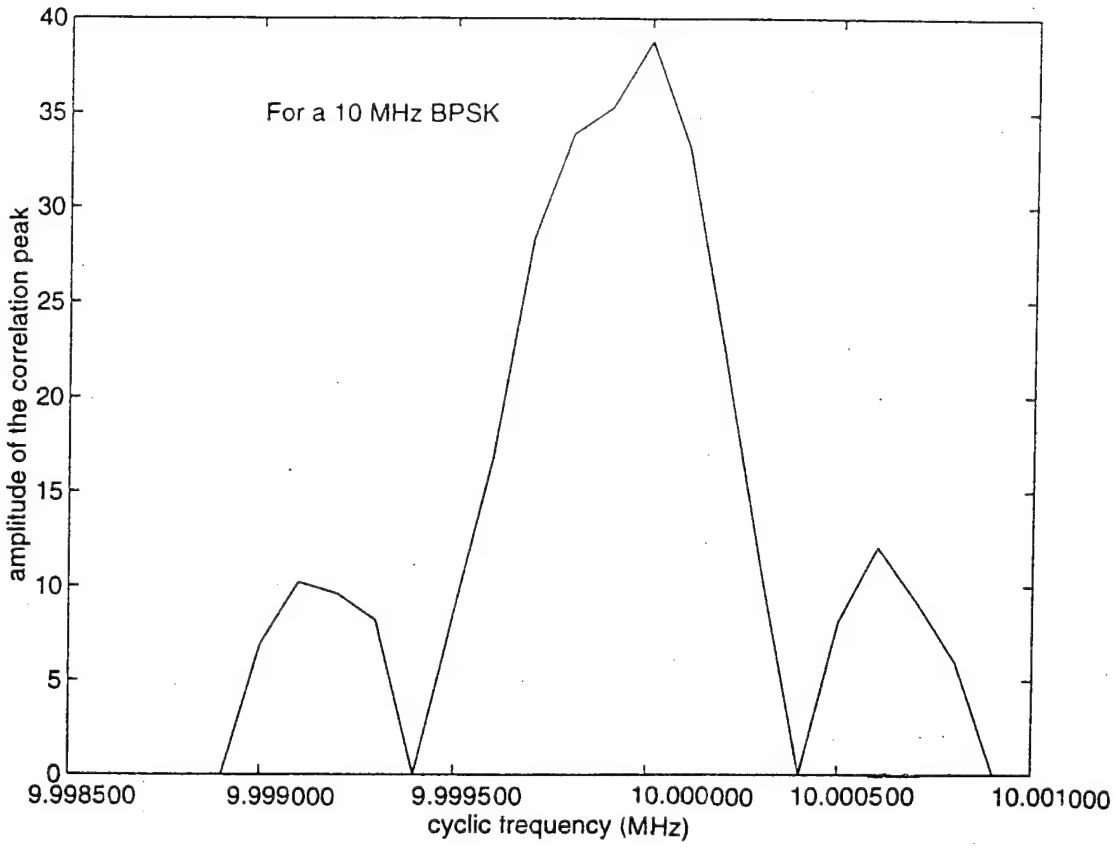

Figure 14: Width of the correlation peak on the cyclic frequency axis α, for a BPSK with a 10 MHz chip rate.

6.0 CONCLUSION

The experimental results presented in this Technical Note clearly demonstrate that the CCC is a powerful algorithm capable of sorting spread spectrum signals sharing the same bandwidth, TDOA and carrier frequency. The characterization of the signals performed by the CCC can be done even in presence of a considerable amount of noise. It also has been demonstrated that an optoelectronic correlator is capable of real-time implementation of the CCC for a particular cyclic frequency. This combination of features makes an optoelectronic implementation of the CCC a very interesting candidate for the ESM of spread spectrum LPI signals processing.

However, many important issues have to be studied and resolved before attempting to design a tactical system. The effects of interference of various nature and of multipath signals has to be established. The effects of non-linearity in the receivers have to be assessed. The resolution achievable on the TDOA axis τ and on the cyclic frequency α has to be measured experimentally and compared to operational requirements. Finally, the dynamic range of the system has to be measured. It may be advantageous to perform some of these studies, at least at the preliminary stage, by simulation.

7.0 REFERENCES

[1] D.L. Nicholson, "Spread Spectrum Signal Design: Low Probability of Intercept and Anti-Jam Systems", Computer Science Press Inc. Rockville, 1988.

[2] R.P. Griffin and J.N. Lee, "Acousto-Optical Wideband Correlator System: Design and Implementation", Applied Optics, vol.33, no.298, p. 6774-6787, 10 Oct. 1994.

[3] N. Brousseau, R. Brousseau, J.W.A. Salt, L. Gutz and M.D.B. Tucker, "Analysis of DNA Sequences by an Optical Time-Integrating Correlator", Applied Optics, vol.31, no.23, p.4802-4815, 10 August 1992.

[4] W. A. Gardner and C.M. Spooner, "Signal Interception: Performance Advantages of Cyclic Feature Detectors", IEEE Transactions on Communications, vol.40, no.1, p.149-159, January 1992.

[5] W.A. Gardner and C. Chen, "Signal-Selective Time Difference of Arrival Estimation for Passive Location of Man-Made Signal Sources in Highly Corruptive Environments, Part I: Theory and Method", IEEE Transactions on Communications, vol.40, no.5, p.1168-1184, May 1992.5.

[6] W.A. Gardner and C.M. Spooner, "Detection and Source Location of Weak Cyclostationnary Signals: Simplifications of the Maximum-Likelihood Receiver", IEEE Transactions on Communications, vol.42, no.6, p.905-916, June 1993.

[7] C.M. Spooner and W.A. Gardner, "Robust Feature Detection for Signal Interception", IEEE Transactions on Communications, vol.42,no.5, p.2165-2173, May 1994.

[8] L. Izzo L. Paura and M. Tanda, "Signal Interception in Non-Gaussian Noise", IEEE Transactions on Communications, vol.40, no.6, p.1030-1037, June 1992.

[9] W. A. Gardner, "Exploitation of Spectral Redundancy in Cyclostationnary Signals", IEEE SP Magazine, p.15-36, April 1991.

[10] W.A Gardner, "Statistical Spectral Analysis: A Non-Probabilistic Theory", Prentice-Hall Inc. 1980, Englewood Cliffs, New Jersey, 1st edition.

[11] W. A. Gardner, "Signal Interception: A Unifying Theoritical Framework for Feature Detection", IEEE Transactions on Communications, vol.36, no.8, p.897-906, August 1988.

[12] A.H. Mudry, "The Exploitation of Spectral Correlation for the Purpose of Signal Search and Detection", Research Note ERL-0572-RN, Electronic Research Laboratory, DSTO Australia.

[13] E. April, "The Advantage of Cyclic Spectral Analysis" (U), DREO TN 92-4, October 1991.

[14] F. Hlawatsch and G.F. Boudreaux-Bartels, "Linear and Quadratic Time Frequency Signal Representations", IEEE SP Magazine, p. 21-67 April 1992.

[15] L. Cohen, "Time Frequency Distributions - A Review", Proceedings of the IEEE, vol.77, no.7 p.941-981, July 1992.

[16] V.S. Kulakov, Y.I. Nikitin, Y.Y Nikiforova and L.N. Preslenev, "Separation of the Clock Frequency of PSK Signals by Means of an Acousto-optic Delay and Multiplication Device", Originally published in Radiotekhnika, no. 6, pp.83-86, 1990.

[17] J.D. Cohen, "Ambiguity Processor Architectures using One-Dimensional Acousto-Optic Transducers", SPIE vol.180 Real-Time Signal Processing II, p.134-142, 1979,

[18] R.J. Sadler and M.R. Buttinger, "Acousto-optic Ambuiguity Function Processor", IEE Proceedings, vol.133, Pt.J. No.1, p.35-46, Feb. 1986.

[19] G. Waxin, M.G. Gazalet, J.M. Rouvaen, E. Bridoux and J.E. Lefebvre, "Acousto-optic Processing: Real-Time Ambiguity Function Processor", Applied Optics, vol.24, no.10, p.1454-1458, 15 May 1985.

[20] W.A. Brown and W.A. Gardner, "Optical Cyclic Spectrum Analysis", Department of Electrical and Computer Engineering, University of California, Davis Report No. SIP4-84-16, Nov. 1984.

[21] D.L. Nicholson, "Cyclostationnary Processing", Notes from a course given at George Washington University, June 1992.

[22] M.W. Casseday, N.J. Berg, I.J. Abramovitz and J.N. Lee, "Wide-band Signal Processing using the Two-Beam Surface Acoustic Wave Acousto-optic Time Integrating Correlator", IEEE Transactions on Sonic and Ultrasonics, vol. SU-28, no. 3, 205-212, 1981.

[23] N.J. Berg, I.J. Abramovitz, J.N. Lee and M.W. Casseday, "A New Surface-Wave Acousto-optic Time Integrating Correlator," Appl. Phys. Lett. 36 (4), 256-257, 1980.

[24] N.J. Berg, M.W. Casseday, A.N. Filipov and J.M. Pellegrino, "A New Multifunction Acousto-optic Signal Processor," in Ultrasonics Symposium, 454-458, 198).

[25] I.J. Abramovitz, N.J. Berg and M.W. Casseday, "Interferometric Surface-Acousto-Optic Time-Integrating Correlator," Ultrasonics Symposium, 483-487, 1980.

[26] N.J. Berg, M.W. Casseday, I.J. Abramovitz and J.N. Lee, "Radar and Communication Band Signal Processing using Time-Integrating Processors," in 1980 International Optical Computing Conference, T. W. Rhodes, ed., Proc Soc. Photo-Opt. Instrum. Eng. 232, 101-107, 1980.

[27] C.S. Tsai, J.K. Wang and K.Y. Liao, "Acousto-optic Time-Integrating Correlators using Integrated Optic Technology," in Real-Time Signal Processing II, Proc. Soc. Photo-Opt. Instrum. Eng. 180, 160-163, 1979.

[28] M. Varasi, A. Vannucci and S. Reid, "Integrated Acousto-optic Correlator using the Proton Exchange Technique," in Optical Information Processing Systems and Architectures, B. Javidi, ed., Proc. Soc. Photo-Opt. Instrum. Eng. 1151, 457-466, 1989.

[29] W.T. Rhodes, "Acousto-optic Signal Processing: Convolution and Correlation," Proc. IEEE, vol.69, p.65-79, 1981.

[30] N. Laouar, J.P. Goedgebuer et R. Ferrière, "Corrélateur opto-électronique analogique pour le traitement en parallèle de signaux de type radar," Onzième colloque GRETSI- Nice, 693-696, 1987.

[31] I.G. Fuss, "Acousto-optic Signal Processor Based on a Mach-Zehnder Interferometer", Appl. Opt., 24, 3866-3871, 1985.

[32] D.A.B. Fogg, "A Compact Bulk Acousto-optic Time Integrating Correlator", Department of Defence of Australia, Technical Report ERL-0323-TR, Nov. 1984.

[33] M.S. Brown, "A Kosters Prism Time-Integrating Acousto-optic Correlator", J. Phys, E:Sci. Instrum. 21, 192-194 (1988).

[34] N. Brousseau and J.W.A. Salt, "Design and Implementation of a Time-Integrating Correlator using Bulk Acousto-Optics Interaction," Defence Research Establishment Note 86-25, 1986.

[35] N.J. Berg and J.N. Lee, "Acousto-optic Signal Processing: Theory and Implementation, 1st ed. (Marcel Dekker Inc., New York and Basel, 1983), Chap.10.

[36] R.A. Sprague and C.L. Koliopoulos, "Time Integrating Acousto-optic Correlator", Appl. Opt., 15, p.89-92, 1976.

[37] C.C. Lee, K.Y. Liao and C.S. Tsai, "Acousto-optic Time-Integrating Correlator using Hybrid Integrated Optics," 1982 IEEE Ultrasonics Symposium, 405-407, 1982.

[38] G. Silbershatz and D. Casasent, "Hybrid Time and Space Integrating Processors for Spread Spectrum Applications", Appl. Opt., 22, 2095-2103, 1983.

[39] D. Casasent, "General Time-, Space-, and Frequency-Multiplexed Acousto-optic Correlator", Appl. Opt., vol.24, 17, 2884-2888, 1985.

[40] F. B. Rotz, "Time-Integrating Optical Correlator", in Active Optical Devices, J. Tracy, ed., Proc. Soc. Photo-Opt. Instrum. Eng. 202, 163-169, 1979.

[41] P. Kellman, "Time-Integrating Optical Signal Processing", Stanford University, Dept. of Electrical Engineering, Ph.D. dissertation, June 1979.

[42] A.P. Goutzoulis and B.V.K. Vijaya Kumar, "Optimum Time-Integrating Acousto-optic Correlator for Binary Codes", Opt. Comm., 48, 393-397, 1984.

[43] I.D. Bondarenko, A.A. Vetrov and Y.V. Popov, "Analysis of the Errors of the Signal Processing Channel of an Acousto-optic Correlator", Sov. J. Opt. Technol.56 (6), 346-349, 1989.

[44] D. Casasent, A. Goutzoulis and B.V.K. Vijaya Kumar, "Time-Integrating Acousto-optic Correlator: Error Source Modelling", Appl. Opt., 23, 3130-3137, 1984.

[45] B.V.K. Vijaya Kumar and J.M. Connelly, "Binarization Effects in Acousto-Optic Correlators", in Optical Information processing Systems and Architectures II, B. Javidi, ed., Proc. Soc. Photo-Opt. Instrum. Eng. 1347, 112-122, 1990.

[46] J.B. Goodell, "Optical Design Considerations for Acousto-Optic Systems", in Advances in Optical Information Processing III, D. R. Pope, ed., Proc. Soc. Photo-Opt. Instrum. Eng. 936, 22-28, 1985.

[47] A. Goutzoulis, D. Casasent and B.V.K. Vijaya Kumar, "Detector Effects on Time-Integrating Correlators Performance", Appl. Opt., 24, 1224-1233, 1985.

[48] N. Brousseau, "Effects of Temperature Chnages on the Output of a Time-Integrating Correlator", DREO TN 93-30.

[49] N. Brousseau and J.W.A. Salt, "A Comparison of Three Pedestal Removal Techniques for an Optical Time-Integrating Correlator", DREO TN 94-16.

[50] N. Brousseau and J.W.A. Salt, "Illumination System for a Time-Integrating Correlator, DREO TN 95-008.

[51] N. Brousseau and J.W.A. Salt, "Analysis and Optimization of the Data Collection Process of a Time-Integrating Correlator", DREO TN 95-5.

[52] N. Brousseau and J.W.A. Salt, "Design and Demonstration of an Acousto-optic Time-Integrating Correlator with Larger Processing Gain", DREO TN 93-24.

DOCUMENT CONTROL DATA

(Security classification of title, body of abstract and indexing annotation must be entered when the overall document is classified)

1. ORIGINATOR (the name and address of the organization preparing the document. Organizations for whom the document was prepared, e.g. Establishment sponsoring a contractor's report, or tasking agency, are entered in section 8.)

DEFENCE RESEARCH ESTABLISHMENT OTTAWA
NATIONAL DEFENCE
SHIRLEYS BAY, OTTAWA, ONTARIO K1A 0Z4

2. SECURITY CLASSIFICATION (overall security classification of the document. including special warning terms if applicable)

UNCLASSIFIED

3. TITLE (the complete document title as indicated on the title page. Its classification should be indicated by the appropriate abbreviation (S,C or U) in parentheses after the title.)

REAL-TIME ANALYSIS OF A SPREAD SPECTRUM ENVIRONMENT WITH AN OPTOELECTRONIC CYCLIC CROSS CORRELATION: PROOF-OF-CONCEPT EXPERIMENT (U)

4. AUTHORS (Last name, first name, middle initial)

N. BROUSSEAU AND J.W.A. SALT

5. DATE OF PUBLICATION (month and year of publication of document)

OCTOBER 1995

6a. NO. OF PAGES (total containing information. Include Annexes, Appendices, etc.)

37

6b. NO. OF REFS (total cited in document)

52

7. DESCRIPTIVE NOTES (the category of the document, e.g. technical report, technical note or memorandum. If appropriate, enter the type of report, e.g. interim, progress, summary, annual or final. Give the inclusive dates when a specific reporting period is covered.)

DREO TECHNICAL NOTE

8. SPONSORING ACTIVITY (the name of the department project office or laboratory sponsoring the research and development. Include the address.)

DEFENCE RESEARCH ESTABLISHMENT OTTAWA
NATIONAL DEFENCE
SHIRLEYS BAY, OTTAWA, ONTARIO K1A 0Z4

9a. PROJECT OR GRANT NO. (if appropriate, the applicable research and development project or grant number under which the document was written. Please specify whether project or grant)

05B02

9b. CONTRACT NO. (if appropriate, the applicable number under which the document was written)

10a. ORIGINATOR'S DOCUMENT NUMBER (the official document number by which the document is identified by the originating activity. This number must be unique to this document.)

DREO TECHNICAL NOTE 95-14

10b. OTHER DOCUMENT NOS. (Any other numbers which may be assigned this document either by the originator or by the sponsor)

11. DOCUMENT AVAILABILITY (any limitations on further dissemination of the document, other than those imposed by security classification)

(XX) Unlimited distribution
( ) Distribution limited to defence departments and defence contractors; further distribution only as approved
( ) Distribution limited to defence departments and Canadian defence contractors; further distribution only as approved
( ) Distribution limited to government departments and agencies; further distribution only as approved
( ) Distribution limited to defence departments; further distribution only as approved
( ) Other (please specify):

12. DOCUMENT ANNOUNCEMENT (any limitation to the bibliographic announcement of this document. This will normally correspond to the Document Availabilty (11). However, where further distribution (beyond the audience specified in 11) is possible, a wider announcement audience may be selected.)

UNLIMITED

UNCLASSIFIED

SECURITY CLASSIFICATION OF FORM

13. ABSTRACT (a brief and factual summary of the document. It may also appear elsewhere in the body of the document itself. It is highly desirable that the abstract of classified documents be unclassified. Each paragraph of the abstract shall begin with an indication of the security classification of the information in the paragraph (unless the document itself is unclassified) represented as (S), (C), or (U). It is not necessary to include here abstracts in both offical languages unless the text is bilingual).

(U) The purpose of this technical note is to present a new algorithm to obtain real-time information for electronic support measures for wideband, low probability of intercept radar and communication signals. This algorithm is the Cyclic Cross Correlation(CCC). It allows the detection, separation and characterization of spread spectrum signals having overlapped spectrum, the same carrier frequency and the same difference of time of arrival. An optoelectronic real-time implementation of the CCC for large bandwidth, spread spectrum signals was performed at the Defence Research Establishment Ottawa using an optical Time-Integrating Correlator(TIC). A description of the real-time optical implementation of the CCC with a TIC and the associated experimental results are presented. An assessment of the potential of this technique for application to radar and communication ESM is also included.

14. KEYWORDS, DESCRIPTORS or IDENTIFIERS (technically meaningful terms or short phrases that characterize a document and could be helpful in cataloguing the document. They should be selected so that no security classification is required. Identifiers, such as equipment model designation, trade name, military project code name, geographic location may also be included. If possible keywords should be selected from a published thesaurus. e.g. Thesaurus of Engineering and Scientific Terms (TEST) and that thesaurus-identified. If it is not possible to select indexing terms which are Unclassified, the classification of each should be indicated as with the title.)

CYCLIC CROSS CORRELATION
TIME-INTEGRATING CORRELATOR
LPI INTERCEPT
NON-LINEAR RECEIVER
LPI DETECTION
CYCLOSTATIONARY SIGNAL PROCESSING